JOURNAL OF MATERIALS SCIENCE 30 (1995) 1455–1461

Fracture behaviour of pressure die-cast aluminium–graphite composites

U.T.S. PILLAI, B.C. PAI, K.G. SATYANARAYANA, A.D. DAMODARAN
Regional Research Laboratory (CSIR), Trivandrum 695019, India

Fracture toughness values of pressure die-cast Al–7Si–3 Mg–5 graphite composites were measured and found to be in the range 8–10 MPa $m^{1/2}$. Detailed microstructure of the composite and the fractured surfaces were examined. Defects such as clusters, agglomerations and segregation of graphite particles, play a dominant role in accelerating the fracture process. In addition, the acicular silicon phase present in the matrix and the casting defects, such as gas and shrinkage porosities, also initiated and accelerated the crack, thus lowering the fracture toughness of the composites.

1. Introduction

The fracture properties of a composite is largely controlled by the type and property of the dispersoid, the nature of the distribution of the dispersoid, the kind of interface that exists between the dispersoid and the matrix, and the properties of the matrix. In addition, the synthesizing route will have strong influence on the fracture properties. Detailed reviews have recently been published [1–5] on the above aspects. The invention of the stir-casting route [6] for synthesizing aluminium-alloy matrix composites has made them an economically viable engineering material. Among the cast composite systems, graphite particle-dispersed aluminium alloy composites have been considered as potential bearing material [7]. The wear [8] and mechanical properties [9] of this composite system have been well characterized. The effect of the size and volume fraction of the dispersed graphite on the fracture toughness and fatigue crack growth in gravity die-cast [10] composites have been studied. The lower fracture toughness values of these composites were attributed to non-uniform distribution of the graphite particles, as well as the casting defects in the composite. By using pressure die casting [11] these defects could be reduced. The present paper presents detailed studies on the fracture process in Al–7Si–3Mg–5 graphite pressure die-cast composites which deals with the morphology of the graphite distribution on the fracture properties.

2. Experimental procedure

The material used in the present investigation was Al–7 Si–3 Mg–5 graphite (wt %) pressure die-cast plates of dimension 120 mm × 120 mm × 12 mm. Processing details of these composite plates using the master composite ingots have been discussed elsewhere [11].

The pressure die-cast composite plates were ultrasonically screened for internal defects and flaws. Defect-free plates (flaw size < 0.1 mm) were chosen for mechanical property evaluation. The tensile, compression and bend tests were carried out using an universal testing machine (Instron) with sample size conforming to ASTM E-8 specification. Impact tests were also carried out using an instrumented Charpy impact tester.

For Mode I fracture toughness tests, the compact tension (CT) specimens prepared (dimensions given in Fig. 1) in accordance with ASTM standard E-399. These specimens were chevron notched because the plane strain condition is well maintained in a chevron-notched ligament [1], which allows the use of smaller specimens than those recommended in ASTM E-399. Even though the chevron-notched specimen does not require fatigue precracking, in the present study, the fracture toughness specimens were fatigue precracked by applying a peak load of 300 kg at 30 Hz on a servohydraulic Instron testing machine Model 8032 of capacity 10 ton (dynamic). These specimens were tested on the above machine in the tensile mode and the load–displacement diagrams were obtained.

Fracture toughness values were measured using Mode I stress intensity factor analysis as described in ASTM E-399 and the conditional fracture toughness, K_q, was calculated using the following relation [12]

$$K_q = \frac{P_q}{BW^{1/2}} f(a/W) \quad (1)$$

where P_q is the load obtained from the load–displacement diagram, B the thickness of the CT specimen, W the width of the CT specimen, a the crack length, and

$$f(a/W) = 29.6(a/W)^{1/2} - 185.5(a/W)^{3/2} + 655.7(a/W)^{5/2} - 1017(a/W)^{7/2} + 639(a/W)^{9/2} \quad (2)$$

0022–2461

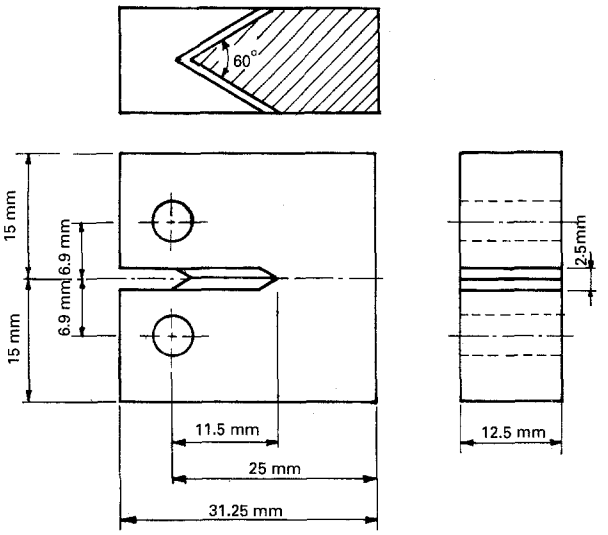

Figure 1 Compact tension specimen used for fracture toughness tests.

The K_q values thus calculated were checked for validity of plane strain fracture toughness criterion

$$B, W - a \geqslant 2.5(K_q/\sigma_{ys}) \quad (3)$$

where σ_{ys} is the yield strength of the composite. It was found that the values do not satisfy the plane strain condition. Thus the K_q values obtained for this composite correspond to conditional fracture toughness but not to plane strain fracture toughness.

Because the microstructural variables, such as distribution of dispersoids, level of porosity, clusters, segregation and agglomeration of particles play an important role in determining the fracture toughness of the composite, the following microstructural studies were carried out on the composites to understand the mechanism involved in the fracture process:

1. optical microstructure of the polished section of the pressure die-cast composite;
2. SEM studies on the fatigue crack path on the CT specimens; and
3. SEM studies on the fractured surface of the tensile and fracture toughness tested specimens.

3. Results and discussions

3.1. Mechanical properties

Table I gives the mechanical properties (ultimate tensile strength (UTS, %), elongation, compressive strength, impact strength and bend strength) of 5 wt % graphite-dispersed aluminium-alloy composite under gravity die-cast and pressure die-cast conditions. It is clear from the results, that pressure die-casting improved the UTS to 135 MPa from 90 MPa without affecting ductility as measured by per cent elongation. The improvement in strength values observed in the pressure die-cast composite is due to decreased defect level (e.g. gas porosities) as shown by density measurement (gravity die-cast 2.65 g cm^{-3}, pressure die-cast 2.67 g cm^{-3}. When cast under similar conditions, the pressure die-cast composite exhibited slightly lower UTS (135 MPa) than the base alloy (145 MPa). Weaker bonding between the particle and the matrix could be the reason for this, as is evident from the microstructure which showed debonding of the particles from the matrix.

3.2. Fracture toughness and its mechanisms

The fracture toughness values of the composites were found to be lower than that of the gravity die-cast base alloy (Table I). The reasons for this were investigated through microstructural studies.

The microstructure of the composite showed three types of particle-related defects as described below.

1. A cluster of particles is defined as a bunch of particles which are loosely bonded and which are not separated during dispersion or subsequent stirring of the melt. The bonding between the particles is either mechanical or pure Van-der-Waal's type.
2. Agglomerations are normally formed by a set of particles coming nearer to each other during stirring or solidification. The particles are normally in contact with each other in certain points/areas only. This happens because of the gas film present over the particles and its tendency to bring particles together [13].
3. Yet another type of particle crowding is called segregation which takes place due to gravity considerations or pushing by the moving solidification front. In this case the particles are individually dispersed in the melt but concentrated at certain regions.

Fig. 2a–c schematically illustrates the above three types of defects.

From the observed graphite particle distribution in the composites and the other matrix defects, the micromechanisms on the fractured surfaces and their effects on the fracture process can be subsequently discussed.

TABLE I Comparison of mechanical properties of LM25 and Al–5 wt % graphite composites cast under gravity and pressure die-cast conditions

Composite system	UTS (MPa)	Elong. (%)	Compressive strength (MPa)	Impact energy (MN)	Bend strength (MPa)	Hardness, BHN	Fracture toughness, K_q (MPa m$^{1/2}$)
Al–5 wt % graphite composite (gravity die-cast) [10]	90	2	–	–	–	–	–
Al–5 wt % graphite composite (pressure die-cast)	135	2	349.8	1.0	369	85–93	8–10
Base alloy pressure die-cast	145	4	483.8	2.5	334	70–80	–
Base alloy gravity die-cast	140	2	–	–	–	70–80	13–15

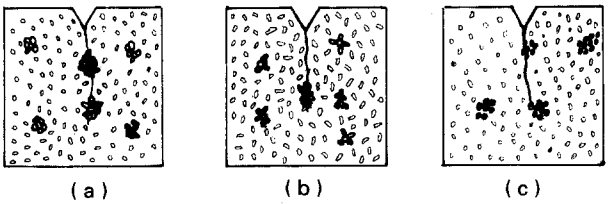

Figure 2 Schematic diagram showing three types of particle distribution: (a) clusters, (b) segregation, (c) agglomeration.

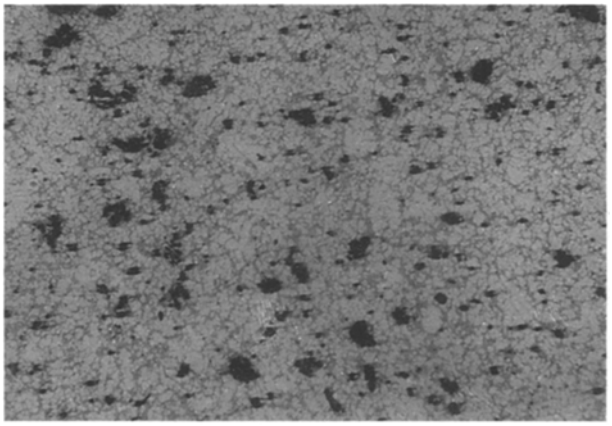

Figure 3 Structure showing clusters of graphite particles in the composite.

3.2.1. Clusters

The distribution of graphite particles in the matrix is predominantly homogeneous and uniform. However, about 3%–5% of the total particles are in the clustered form (Fig. 3). When a growing crack approaches a cluster (see Fig. 2a), it finds an easy path to travel though the cluster without taking any additional load. Because there is no matrix material inside the cluster, the degree of plastic constraint within the clusters could be much higher than the rest of the matrix as a result of the increase in triaxial stress state during deformation [4].

3.2.2. Agglomeration

The agglomeration of particles observed in the pressure die-cast aluminium-graphite composite is shown in Fig. 4. Distribution of agglomeration of particles in the matrix can be considered as a damaged or defective particle. This defective particle can significantly degrade the mechanical properties of the composite by nucleating cracks at the surface or in the core [14]. Because the particles are notch sensitive, the stress that is required to break the agglomeration or the stress required for the extension of a growing crack through the agglomeration, is much less than that predicted from the case of an ideal particle. Thus the fracture process becomes accelerated, if the path encounters an agglomeration.

3.2.3. Segregation

Fig. 5 shows the typical appearance of graphite particle segregation in the aluminium matrix. Segregation

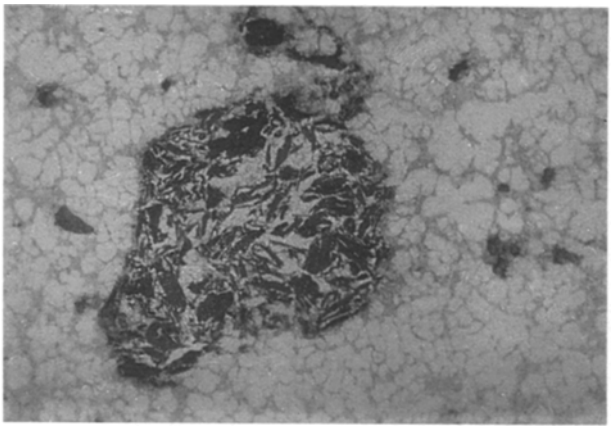

Figure 4 Typical agglomeration of graphite particles present in the composite.

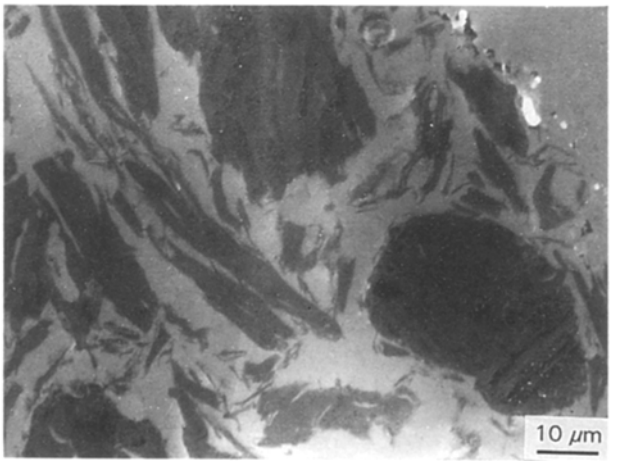

Figure 5 Segregation of graphite particles in the composite.

of particles not only leads to a higher volume fraction but also reduces the interparticle spacing. The combined effect of the nucleation and growth of crack within the segregation increases the fracture process, thus reducing the toughness of the composite. During pressure die-casting, because of the faster cooling rate, the solidification-aided graphite particle segregation is minimized; however, in the present case, improper dissolution of the master composite has led to small amounts of segregation. This accounts for about 10 vol % of the total graphite particles in the segregated condition.

3.2.4. Larger size particles

In addition to the above-mentioned particle defects, the presence of a few larger sized (50–100 μm) graphite particles also contributed to the decrease in the fracture toughness values. As reported earlier [3], as the particle size increases above a certain diameter, toughness decreases and the proportion of the cracked particles increases. This is substantiated by the existence of cracks in the fractured particles (Fig. 6). In addition, the larger the size of the particles, the more the total path is cleaved by the particles. This means that a larger proportion of the composite fails in a brittle manner, which is also observed from the fractograph.

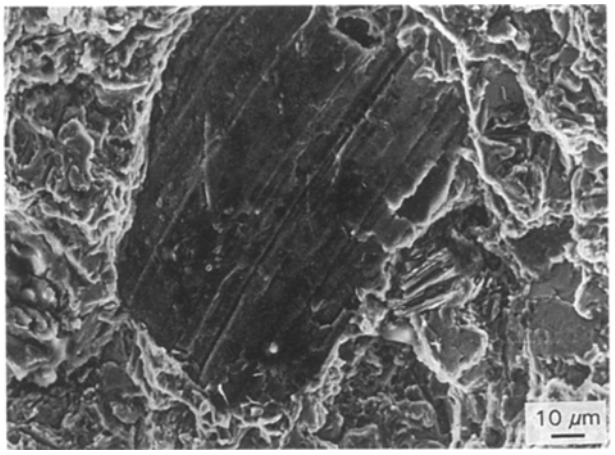

Figure 6 Cracks on the fractured particle and the brittle type of fracture around the larger particles (≃ 100 μm size).

3.2.5. Intermetallics and other defects

In general, intermetallics, inclusions, precipitates, etc. present in the matrix can influence the fracture toughness of the composite material [14]. The microstructure (Fig. 7a–c) revealed higher concentration of silicon needles along the grain boundary (Fig. 7a) and at the graphite–matrix interface (Fig. 7b). This needle-shaped silicon phase initiated the crack (see Fig. 7c) around the graphite particles and at the interface, due to the increased stress concentration resulting from the tip of the silicon phase. Attempts to modify the shape of the silicon phase from acicular to a more spherical one by suitable heat treatment failed in the present context, due to the appearance of blisters on the surface of the pressure die-cast samples during such treatment. In addition, the microshrinkage porosities present in the composites (Fig. 7d) also contribute to the lowering of the fracture toughness of the composite.

3.3. Studies on crack path

SEM studies carried out on the polished surface of the fatigue-cracked, but not fractured, CT specimen further strengthened the above observations.

1. The growing crack finds an easy path along the larger particles (Fig. 8).
2. The appearance of the sharp crack tip (see Fig. 8) confirms the absence of crack blunting.
3. In addition to the primary crack, many secondary and tertiary cracks are also seen in the matrix (see Fig. 9a). These short microcracks are associated with the clusters, agglomeration and segregation of graphite particles as well as silicon phase present in the matrix. Similar observations were reported by Folm and Arsenault for Al–SiC_p composites [4] where cracking took place in the matrix ahead of the crack tip by forming a damaged zone, and the crack growth

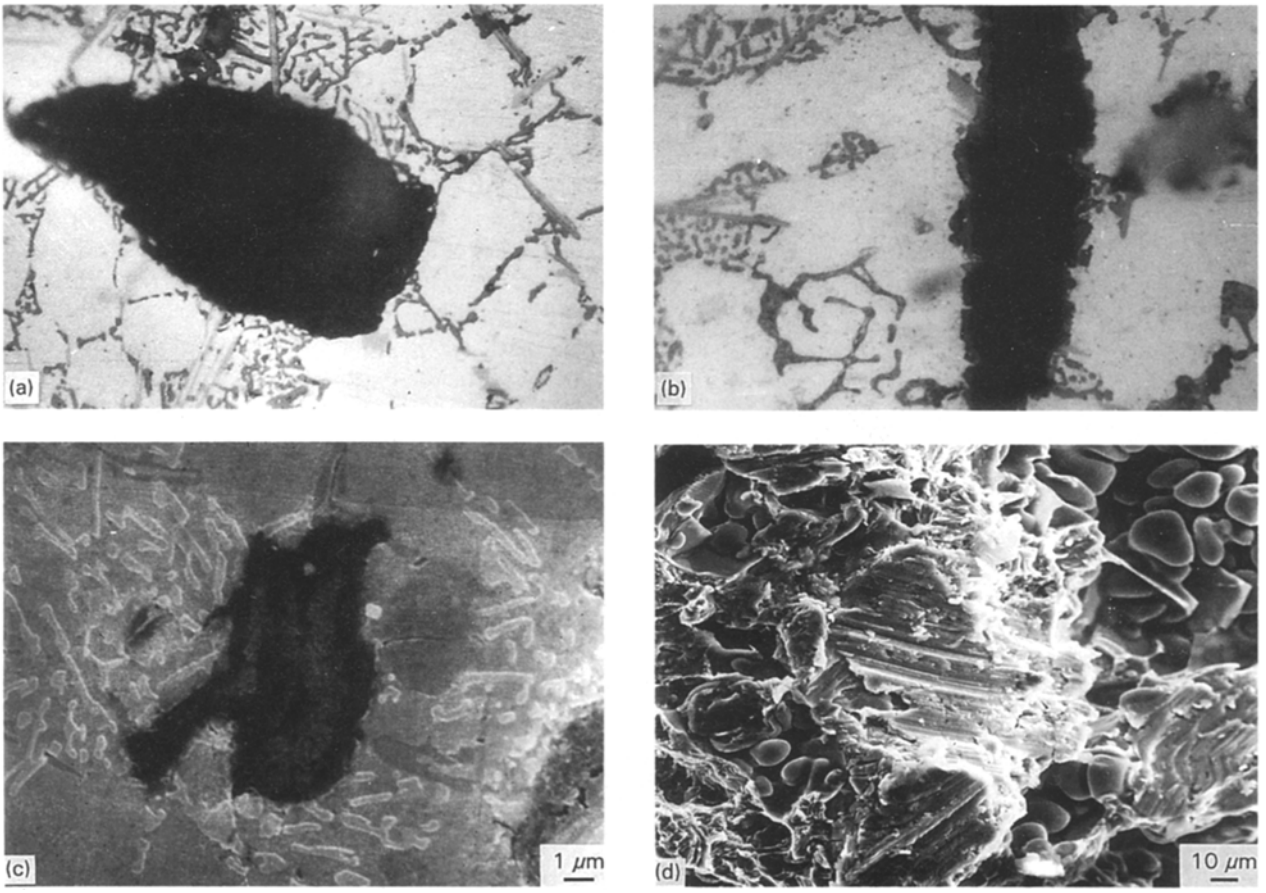

Figure 7 Silicon phase and other intermetallics around the graphite particles. (a) Silicon phase along the grain boundary; (b) silicon phase around the graphite particles; (c) silicon phase initiating cracking along the graphite particle; (d) microfractograph showing the shrinkage porosities.

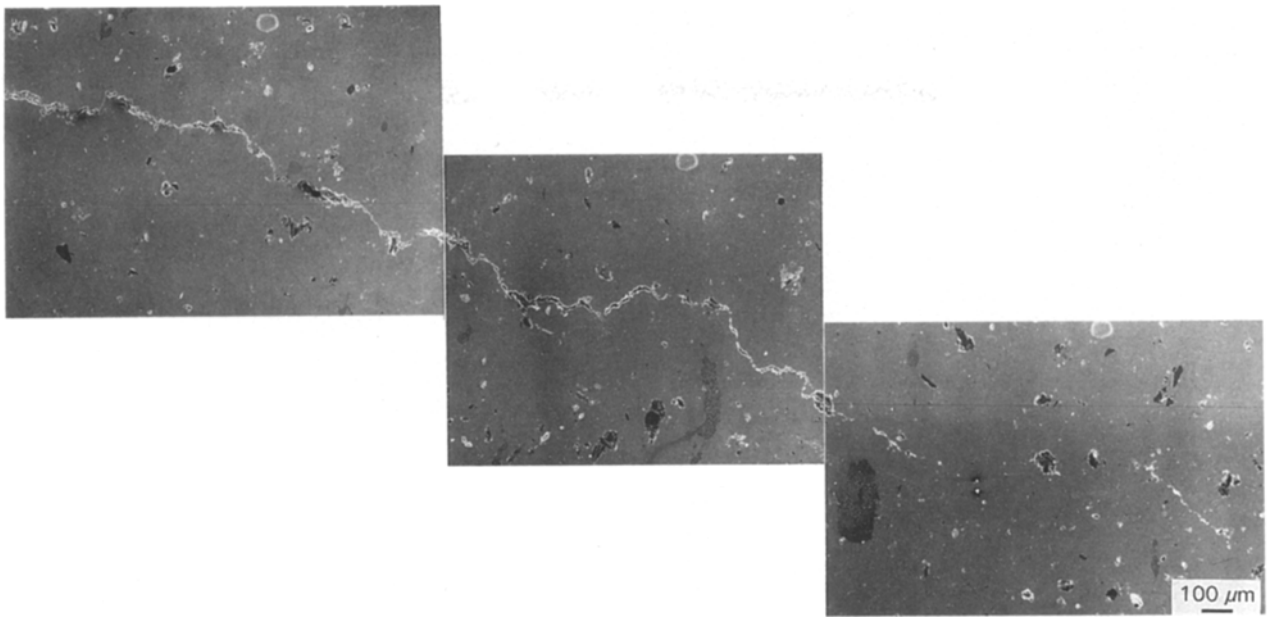

Figure 8 The crack path on the fatigue cracked fracture toughness specimen.

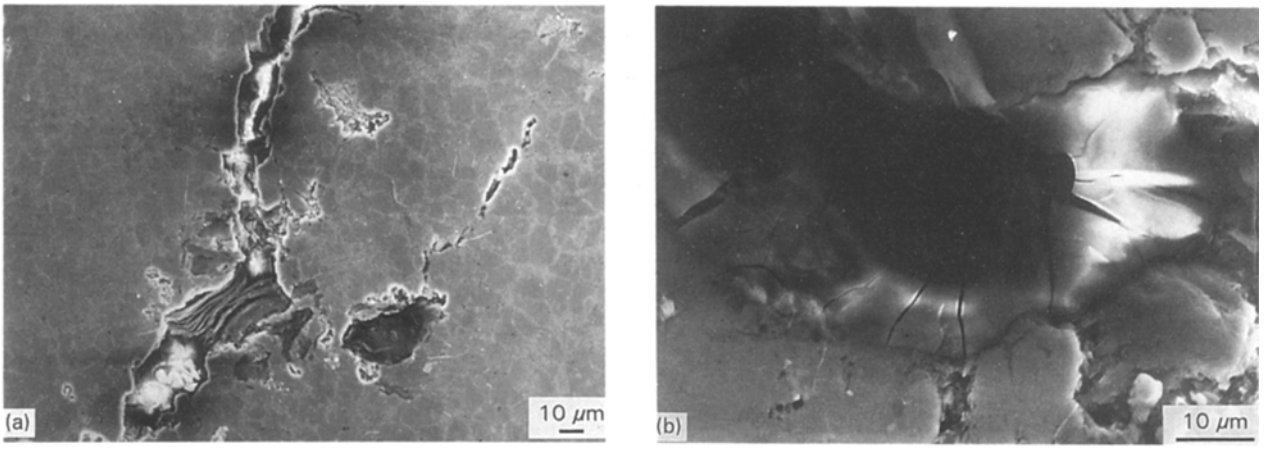

Figure 9 Crack path showing (a) secondary and tertiary cracks along with the primary crack, as well as the presence of voids on the crack path, (b) a number of microcracks joining to form the primary crack.

occurred by connecting these continuous short microcracks (secondary cracks) (see Fig. 9b).

4. The presence of voids seen on the fracture path (see Fig. 9a) confirms that the fracture occurred by nucleation, growth and coalescence of voids giving rise to a ductile fracture mode of failure.

3.4. Microfractography

SEM observations of the fractured surfaces of the CT specimens, shown in Fig. 10a–e, revealed that the fracture occurred in the composite in a ductile mode, even though they exhibited limited ductility on the macroscopic scale (see Fig. 10a). Similar observations have been reported by other researchers for Al–SiC [4], Al–Al_2O_3 [3], Al–graphite [10] and Al–zircon [10] composites. These fractographs suggest that the fracture toughness of this composite was mainly controlled by the particles present in the matrix and the cracks nucleating near the weak interface because of local stress concentration. Once the local stress exceeds the interfacial bond strength, crack extension, as well as particle decohesion occurs [15]. The cracked particles suggested that these particles participated in the fracture process. Fig. 10b shows the interfacial cracks as well as particle cracking. Evidence of debonding is seen with a clear gap between the particles and the matrix (see Fig. 10c) and, in some cases, cavities can be seen, indicating the removal of particles from the matrix (Fig. 10d). In addition, a number of matrix cracks and shrinkage porosities are also observed on the fracture surface (Fig. 7d).

Attempts were made to observe the details of the fracture modes due to clusters, segregation and decohesion of the graphite particles on the fracture surfaces, including the matching pair of fracture surfaces. However, these efforts were not completely successful because of graphite particles falling out of the fractured surfaces during handling.

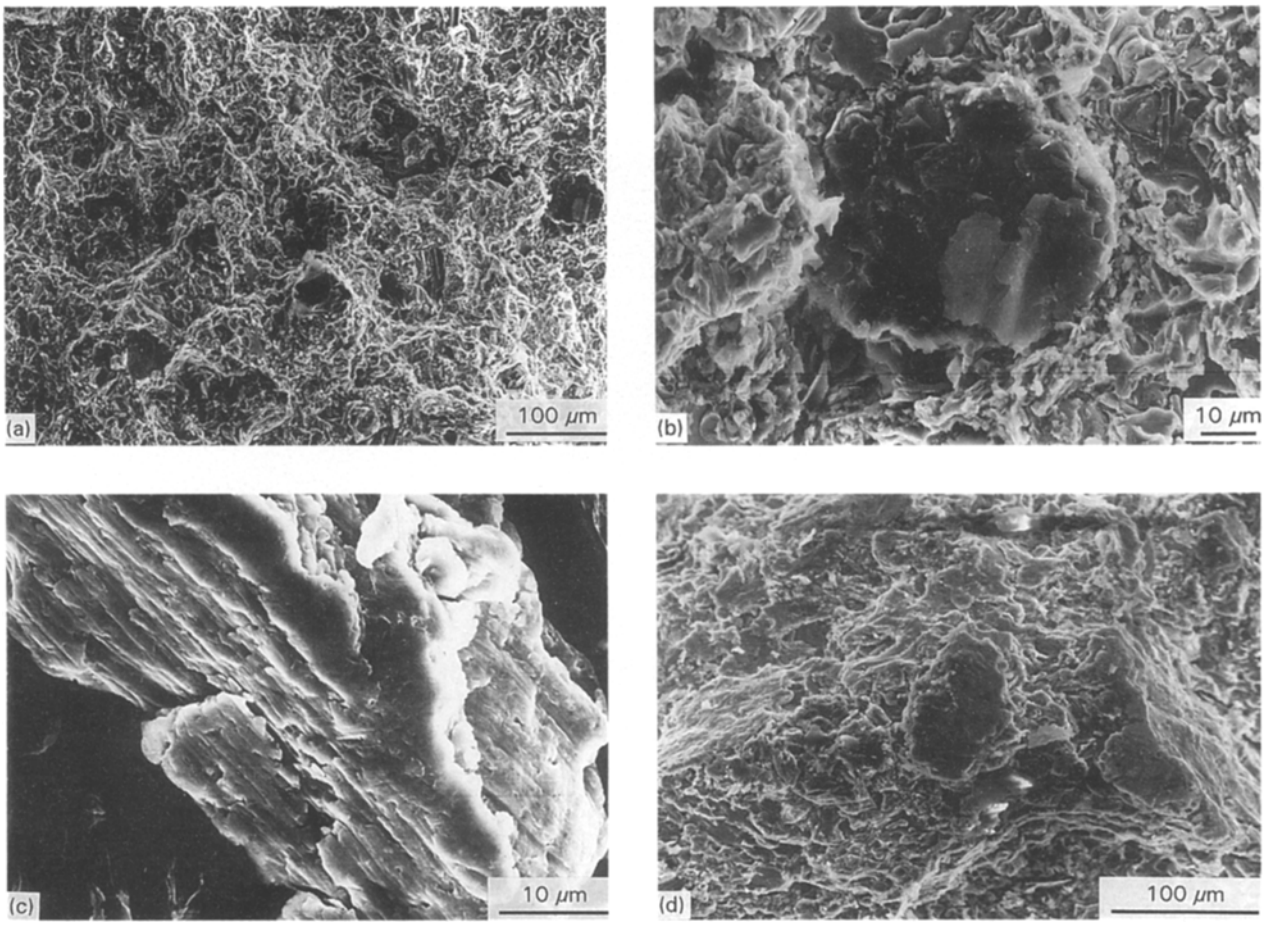

Figure 10 Fractured surfaces showing (a) ductile mode of fracture, (b) interfacial cracks as well as particle cracking, (c) debonding of a single particle, and (d) cavities, indicating removal of particles from the matrix.

In summary, the particle distribution (clusters, agglomeration and segregation) plays an important role in the fracture process, with the order of preference, the worst being clusters (because of its inherent nature) followed by agglomeration and then segregation. In addition, the larger particles as well as the presence of silicon needles at the graphite–matrix interface, also initiate and accelerate the crack growth.

4. Conclusions

1. The strength properties of the pressure die-cast plates are superior to those of the gravity die-cast samples.

2. Fracture toughness values evaluated by testing the precracked fracture toughness specimens from the pressure die-cast composites were found to be in the range 8–10 MPa $m^{1/2}$.

3. Fracture toughness of this composite is primarily controlled by graphite particle distribution, i.e. clusters, agglomeration and segregation, as well as silicon phase present in the matrix.

4. Larger particles can reduce the fracture toughness, because the crack finds an easy path through them.

5. The fracture surface of the composite exhibits the combined effect of debonding and cracking of particles and the matrix cracks. In addition to this, shrinkage and gas porosities are also seen.

Acknowledgements

The authors thank Professor E. S. Dwaraka Dasa and Mr Shashidhara, Department of Metallurgy, Indian Institute of Science, Bangalore, for extending the fracture toughness test facility, and Mrs Prasannakumari, Mr S. G. K. Pillai and Mr P. Vijayakumar for SEM, optical microscopic and photographic work, respectively.

References

1. A. MORTENSEN, Proceedings of the ASM International Conference on "Fabrication of Particulates, Reinforced Metal Composites", Montreal, Canada, September (1990), edited by J. Masounave and F. G. Hamel (ASM International, Materials Park, OH, 1990) p. 217.
2. I. A. IBRAHIM, F. A. MOHAMED and E. J. LAVERNIA, *J. Mater. Sci.* **26** (1991) 1137.
3. S. V. KAMAT, J. P. HIRTH and R. MEHRABIAN, *Acta. Metall.* **37** (1989) 2395.
4. Y. FOLM and R. J. ARSENAULT, *ibid.* **37** (1989) 2413.,
5. ZHURI WANG and RUBY J. ZHANG, *Metall. Trans.* **22A** (1991) 1585.
6. P. K. ROHATGI, R. ASTHANA and S. DAS, *Int. Metals Rev.* **31**(3) (1986) 115.
7. S. BISWAS, A. SANTHARAM, N.A.P. RAO, K. NARAYANASWAMY, P. K. ROHATGI and S. K. BISWAS, *Tribol. Int.* **8** (1980) 171.
8. P. K. ROHATGI, S. RAY and Y. LIU, *Int. Metals. Rev.* **37**(3) (1992) 129.
9. B. S. MAJUMDHAR, A. H. YEGNESWARAN and P. K. ROHATGI, *Mater. Sci. Eng.* **68** (1984) 85.

10. U. T. S. PILLAI, PhD thesis, IIT, New Delhi (1986).
11. U. T. S. PILLAI, V. S. KELUKUTTY, B. C. PAI and K. G. SATYANARAYANA, *Mater. Sci. Eng.* **A169** (1993) 93.
12. D. BROEK, "Elementary Engineering Fracture Mechanics", (Martinus Nijhoft, Bordrecht, 1986) p. 181.
13. GEETHA RAMANI, R. M. PILLAI, B. C. PAI and T. R. RAMA MOHAN, *Composites* **22** (1991) 143.
14. T. G. NEIH, R. A. RAINEN and D. J. CHELLMAN, in "Proceedings of the 5th International Conference on Composite Materials-ICCMV", edited by W. C. Harrigan J. Strife and A. K. Dhingra, San Diego, CA (1985) (The Metallurgical Society, AIME, Warrendale, PA, 1985) p. 825.
15. P. MUMMERY and B. DERBY, *Mater. Sci. Eng.* **A135** (1991) 221.

Received 17 January
and accepted 11 August 1994